

X-ray emission from the luminous O-type subdwarf HD 49798 and its compact companion

S. Mereghetti¹, N. La Palombara¹, A. Tiengo^{2,1,4}, N. Sartore¹, P. Esposito¹, G.L. Israel³, L. Stella³

¹ INAF, Istituto di Astrofisica Spaziale e Fisica Cosmica Milano, via E. Bassini 15, I-20133 Milano, Italy

² IUSS, Istituto Universitario di Studi Superiori, piazza della Vittoria 15, I-27100 Pavia, Italy

³ INAF, Osservatorio Astronomico di Roma, via Frascati 33, I-00040 Monteporzio Catone, Italy

⁴ INFN, Istituto Nazionale di Fisica Nucleare, Sezione di Pavia, via Bassi 6, I-27100 Pavia, Italy

Received February 9, 2013 / Accepted April 4, 2013

ABSTRACT

The X-ray source RX J0648.0–4418 is the only confirmed binary system in which a compact object, most likely a massive white dwarf, accretes from a hot subdwarf companion, the bright sdO star HD 49798. The X-ray emission from this system is characterized by two periodic modulations caused by an eclipse, at the orbital period of 1.55 d, and by the rotation of the compact object with a spin period of 13.2 s. In 2011 we obtained six short *XMM-Newton* observations centered at orbital phase 0.75, in order to study the system during the eclipse, and spaced at increasingly long time intervals in order to obtain an accurate measure of the spin-period evolution through phase-connected timing. The duration of the eclipse ingress and egress, ~ 500 s, indicates the presence of an X-ray emitting region with dimensions of the order of a few 10^4 km, surrounding the pulsar and probably due to scattering in the companion's wind. We derived an upper limit on the spin-period derivative $|\dot{P}| < 6 \times 10^{-15} \text{ s s}^{-1}$, more than two orders of magnitude smaller than the previously available value. Significant X-ray emission is detected also during the 1.2 hours-long eclipse, with a luminosity of $\sim 3 \times 10^{30} \text{ erg s}^{-1}$. The eclipse spectrum shows prominent emission lines of H- and He-like nitrogen, an overabundant element in HD 49798. These findings support the suggestion that the X-ray emission observed during the eclipse originates in HD 49798 and that the processes responsible for X-ray emission in the stellar winds of massive O stars are also at work in the much weaker winds of hot subdwarfs.

Key words. Subdwarfs – X-rays: binaries – Stars: winds – Stars: individual: HD 49798

1. Introduction

The X-ray source RX J0648.0–4418 is one of the very few known binaries composed of a hot subdwarf and a compact object. The optical component is the bright blue star HD 49798, classified as a subdwarf of spectral type O6, with effective temperature $T_{\text{eff}} = 47,500$ K, and surface gravity $\log g = 4.25 \pm 0.2$ (Kudritzki & Simon 1978). Early spectroscopic observations showed a dominance of He and N lines and an underabundance of C and O, as well as radial velocity variations pointing to a binary nature, that was later confirmed through the discovery of an orbital period of 1.5477 d (Thackeray 1970).

The nature of the companion of HD 49798, undetectable in the optical band due to the presence of the much brighter sdO star, could be revealed only in 1996, thanks to the *ROSAT* discovery of soft X-rays pulsed with a period of 13.2 s (Israel et al. 1997), compatible only with either a neutron star or a white dwarf. While with the *ROSAT* data it was not possible to discriminate between these two possibilities, more recent observations carried out with *XMM-Newton* showed that the compact object is most likely a massive white dwarf (Mereghetti et al. 2009).

For a distance of 650 pc¹ (Kudritzki & Simon 1978), the observed X-ray flux corresponds to a bolometric X-ray luminosity of $\sim 10^{32} \text{ erg s}^{-1}$. Taking into account the relatively well known properties of the stellar wind of HD 49798 (Hamann 2010), it

can be shown that this luminosity is consistent with that expected for Bondi-Hoyle accretion onto a white dwarf, but too small for an accreting neutron star (Mereghetti et al. 2011). The presence of an X-ray eclipse lasting ~ 1.2 h indicates that the system is seen at high inclination $i \sim 82^\circ$. The masses of the two components have been dynamically measured through X-ray pulse timing and the spectroscopically determined optical mass function: they are $M_{\text{opt}} = 1.50 \pm 0.05 M_\odot$ for the subdwarf and $M_X = 1.28 \pm 0.05 M_\odot$ for its companion (Mereghetti et al. 2009). Currently, HD 49798 is well within its Roche-lobe and mass transfer through wind accretion proceeds at a low rate of $\sim 8 \times 10^{-13} M_\odot \text{ yr}^{-1}$. After the formation of a CO core, the subdwarf will expand and transfer He-rich material through Roche-lobe overflow at a higher rate. If the compact object is indeed a massive white dwarf, it may reach the Chandrasekhar limit and either explode as a type Ia supernova (Wang & Han 2010) or form a fast-spinning neutron star through an accretion-induced collapse. This could be a way to create a millisecond pulsar directly, i.e. without a spin-up phase in a low mass X-ray binary.

During the only X-ray eclipse observed in May 2008 some faint X-ray emission was detected, but it could not be studied in detail with the short available exposure. We therefore carried out a series of time constrained *XMM-Newton* observations with the main objective to study the X-ray emission during the eclipse of this unique binary.

Send offprint requests to: S. Mereghetti, sandro@iasf-milano.inaf.it

¹ The poorly constrained Hipparcos parallax of 1.16 ± 0.63 mas (Perryman & ESA 1997) is consistent with this distance.

Table 1. Log of the 2011 *XMM-Newton* observations of RX J0648.0–4418.

Observation	Date	MJD start	MJD end	Orbital Phase ^a	Duration pn/MOS (ks)
1	2011 May 02	55683.550	55683.764	0.685–0.824	17.0 / 18.5
2	2011 Aug 18	55791.876	55792.069	0.677–0.803	15.0 / 16.6
3	2011 Aug 20	55793.458	55793.624	0.699–0.808	11.8 / 14.3
4	2011 Aug 25	55798.040	55798.267	0.660–0.806	18.0 / 19.6
5	2011 Sep 03	55807.349	55807.542	0.675–0.801	15.0 / 16.6
6	2011 Sep 08	55811.997	55812.189	0.678–0.802	15.0 / 16.6

^a Phase 0.75 corresponds to the middle of the eclipse.

2. Observations and data reduction

Six *XMM-Newton* observations of HD 49798/RX J0648.0–4418 were performed between May and September 2011. Each observation lasted about 15 ks and included orbital phase 0.75, corresponding to the center of the X-ray eclipse (see Table 1 for details). Here we report on the results obtained with the EPIC (0.15–12 keV) and RGS (0.3–2.5 keV) instruments. The data were processed using version 11 of the *XMM-Newton* Standard Analysis Software. Some observations showed the presence of short time intervals affected by a high flux of soft protons, which caused a slight increase in the particle background at high energies. We verified that our spectral results are insensitive to the inclusion or exclusion of such time intervals and therefore decided to use the whole data set.

EPIC consists of two MOS and one pn CCD cameras (Turner et al. 2001; Strüder et al. 2001). During all the observations the three cameras were operated in Full Frame mode (time resolution of 73 ms and 2.6 s for pn and MOS, respectively) and with the medium optical blocking filter. For the timing analysis we used a circular extraction region with radius of 30". The photon arrival times were converted to the Solar System barycenter reference frame, by using the coordinates R.A. = 6^h 48^m 04.7^s, Decl. = –44° 18' 58.4" (J2000), and corrected for the orbital motion of the source with the system parameters given in Mereghetti et al. (2011). In order to avoid possible contamination from a nearby source (located 70" away), we extracted the counts for the EPIC spectral analysis from a circle of 20" radius, which corresponds to an enclosed energy fraction of ~80% and ~75% for the pn and MOS, respectively. The spectra were rebinned so as to have at least 30 counts per energy channel. The background spectra were extracted from source-free regions on the same chip as the target. The spectral fits were done with version 12.7 of the XSPEC package.

The RGS instrument (den Herder et al. 2001) has a significantly smaller effective area than EPIC, but its excellent spectral resolution makes it particularly sensitive to narrow emission lines even in relatively faint X-ray sources like RX J0648.0–4418. We extracted the first order spectra and response matrices from both RGS units in each observation using a source extraction region corresponding to 80% of the point spread function in the cross dispersion direction. This region is smaller than that typically adopted in RGS spectral analysis and was chosen in order to minimize the contamination from the nearby source mentioned above (very likely an active star), which shows prominent X-ray emission lines. The source and background spectra and the response matrices of the seven observations were combined together to obtain a cumulative spectrum for each RGS camera. These spectra were rebinned in order to have at least 20 counts per energy channel.

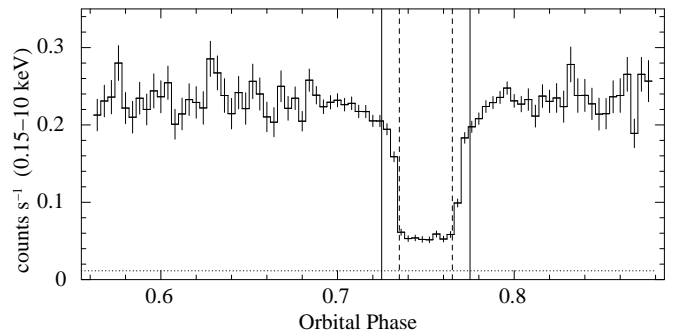


Fig. 1. Light curve of RX J0648.0–4418 in the 0.15–10 keV energy range folded at the orbital period in bins of 535 s. The light curve has been obtained by summing the pn and MOS data of the six observations of 2011 and of the 2008 observation. The horizontal line indicates the background level. The vertical lines delimit the phase intervals used for the spectral analysis.

3. Data analysis and results

The 0.15–10 keV light curve obtained by folding the 2008 and 2011 EPIC data (pn plus MOS) at the $P = 1.547667$ d orbital period is shown in Fig. 1. The horizontal line shows the level of the background and the vertical lines delimit the time intervals used for the spectral analysis described below.

3.1. Emission during the eclipse

We start by examining the spectrum of the X-rays emitted during the eclipse, which can now be studied in detail thanks to the seven-fold increase in exposure time compared to the previous observations. The spectrum of the single eclipse observed in May 2008 (~4 ks exposure) was well fit by either a thermal bremsstrahlung ($kT_{\text{Br}} = 0.55$ keV) or a power law (photon index = 2.8), but these simple models are rejected by the inclusion of the new data. In fact no simple single-component model can fit the total EPIC spectrum (2008 + 2011, 0.2–10 keV) extracted from the 0.735–0.765 phase interval (vertical dashed lines in Fig. 1). In all cases the reduced χ^2 values are unacceptable (2.8, 7.1 and 4.3 for absorbed power law, blackbody and bremsstrahlung, respectively) and the residuals from the best-fit model show the presence of a significant excess at 0.4–0.5 keV, probably due to a blend of unresolved emission lines (lower panel of Fig. 2). A good fit is obtained with a power-law plus two narrow lines² with energies fixed at $E_1 = 0.43$ keV and $E_2 = 0.50$ keV, corresponding to emission from NVI and NVII ions. The best-fit spectrum of the pn data is shown in Fig. 2. Fully consistent results were obtained with the MOS spectra. The best-fit

² We fixed the width to $\sigma = 0$ keV, which corresponds to the assumption of an intrinsic width smaller than the instrumental resolution.

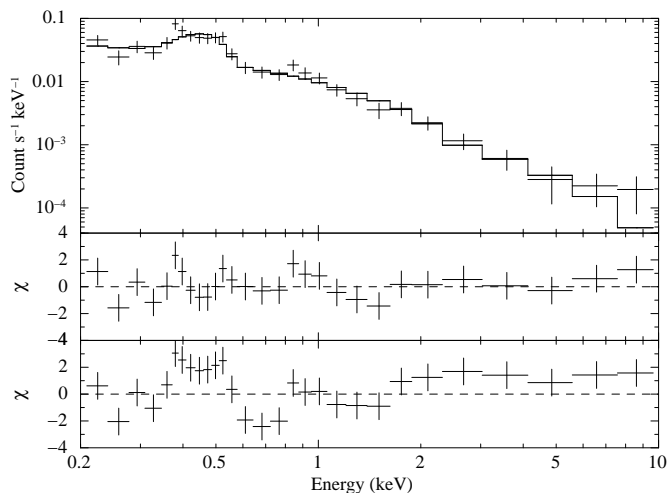


Fig. 2. X-ray spectrum during the eclipse (pn data). Top panel: data and best-fit model consisting of an absorbed power law and two Gaussian emission lines. Middle panel: residuals of the best-fit model. Bottom panel: residuals obtained using only an absorbed power law.

parameters obtained by the joint pn and MOS analysis are given in Table 2.

After background subtraction, the RGS spectra corresponding to the eclipse phases contain only about 100 counts in total, consistent with what expected from the best-fit EPIC model. An excess of counts is present at the energy of the most intense line. Fitting this excess with a narrow line with energy fixed at 0.431 keV, yields a line flux of $(1.1 \pm 0.7) \times 10^{-5}$ ph cm $^{-2}$ s $^{-1}$. No excess is seen at 0.5 keV, but this is not surprising considering the small photon counting statistics of the RGS spectra and the low flux estimated with EPIC for this line.

To explore the possibility that the X-rays during the eclipse originate in HD 49798 we tried a fit with a combination of plasma emission models with different temperatures. The spectra of a large sample of O-type stars detected with *XMM-Newton* were well described by the sum of up to three thermal components³ with temperatures from ~ 0.1 to a few keV (Nazé 2009). Using this model with plasma Solar abundances we could not obtain a good fit to the pn spectrum. This is not surprising considering the overabundances of N and He in this system (Kudritzki & Simon 1978; Hamann 2010).

A good fit (reduced $\chi^2 = 0.86$ for 23 d.o.f., Fig.3) was instead obtained with the sum of three thermal plasma models with the He and N abundances set to the values observed in HD 49798 (mass fractions of $X_{\text{He}} = 0.78$ and $X_{\text{N}} = 0.025$). The derived temperatures are $kT_1 \sim 0.14$, $kT_2 \sim 0.7$, $kT_3 = 5$ keV⁴. The 0.2–10 keV flux is 7×10^{-14} erg cm $^{-2}$ s $^{-1}$. This model is also consistent with the RGS data.

3.2. Emission out of the eclipse

We extracted from the six 2011 observations the spectra excluding the phase interval 0.725–0.775 (solid lines in Fig.1). After checking that they did not show statistically significant differences in flux or spectral parameters, we summed them to obtain a total spectrum for each camera. Assuming that the X-ray emis-

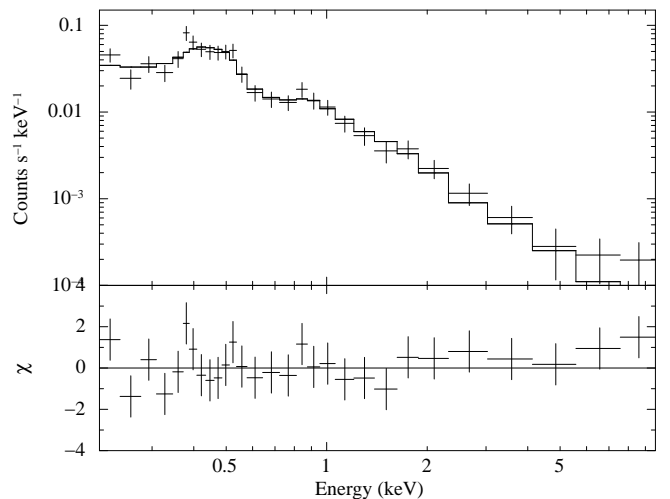


Fig. 3. Spectrum during the eclipse (pn data) fit with three thermal plasma emission models. Bottom panel: residuals from the best-fit model.

sion observed during the eclipse is a steady component present at all orbital phases, as it was done also in Mereghetti et al. (2011) for the 2008 data, we include in the fit the eclipse model with parameters fixed at the values of Table 2. In addition, two other components are required to fit the data: a blackbody plus either a power law or a bremsstrahlung, yielding the results summarized in Table 3. Having included a more accurate description of the eclipse spectrum compared to our previous works, we obtain now slightly different best-fit values for the non-eclipsed emission. In particular, the blackbody component derived in Mereghetti et al. (2011) had a higher temperature (~ 40 eV) and a smaller emitting radius (~ 18 km), compared to the updated values reported here.

By summing the 2008 and 2011 RGS data corresponding to the uneclipsed emission we obtained a spectrum with total exposure time of 129 ks. This spectrum suggests that the line at 0.431 keV is present also out of the eclipse, since it shows an excess with flux of $(0.65 \pm 0.21) \times 10^{-5}$ ph cm $^{-2}$ s $^{-1}$ (i.e. a significance $\sim 3\sigma$).

3.3. Eclipse duration and shape

We fit the folded orbital light curve with a piecewise function consisting of two constants (the eclipse and out-of-eclipse values) connected by linear functions to model the eclipse ingress (between Φ_1^i and Φ_2^i) and egress (between Φ_1^e and Φ_2^e). We assumed a symmetric profile, i.e. the same duration for the ingress and egress. With a fit to the pn light curve in the 0.15–0.5 keV energy range, where the signal-to-noise ratio is maximum, we obtained a total eclipse duration ($\Phi_1^e - \Phi_2^i$) of 4311 ± 52 s and a duration of 525 ± 49 s for the eclipse ingress/egress. We repeated the same analysis after dividing the 0.15–0.5 keV counts into two energy bands with roughly the same number of counts without finding statistically significant evidence for any energy dependence of the eclipse parameters.

The gradual ingress and egress phases can be explained by either assuming that the X-rays originate from an extended region around the compact object or that they are gradually absorbed in the densest regions of the wind close to the surface of HD 49798. In the hypothesis of absorption in the atmosphere/wind of HD 49798, we would expect to observe some energy dependence in the orbital light curves near the eclipse.

³ Model MEKAL in XSPEC.

⁴ The hottest component is required to account for the significant emission above $E > 5$ keV. Its temperature is very poorly constrained by the data, so we fixed it at the plausible value $kT_3 = 5$ keV.

As mentioned above, the comparison of the eclipse profiles in two energy bands was inconclusive, so we attempted to test this hypothesis by analyzing the spectra of the ingress and egress phases as follows.

We summed all the EPIC/pn spectra extracted from the phase intervals 0.725–0.735 and 0.765–0.775 and tried to fit the resulting spectrum by varying in two different ways the blackbody plus power-law model of the non-eclipsed emission. This was done a) by introducing a multiplicative factor (to simulate the gradual occultation of an extended source) and b) by keeping only the column density as free parameter (to check whether the flux decrease can be explained only by absorption). In both cases all the other parameters were kept fixed at their best-fit values of the non-eclipsed emission and the assumed constant eclipse spectrum (Table 2) was included. The resulting values of reduced $\chi^2 = 0.99$ and $\chi^2 = 1.42$, respectively, favor the first interpretation.

3.4. Spin period evolution

The pulsations at the spin period of 13.2 s are clearly detected at consistent values in each of the six observations carried out in 2011. To improve the accuracy of the period determination, we performed a joint timing analysis of the 2011 pn data in the soft X-ray band (<0.5 keV) as follows. We first phase-connected the two most closely spaced observations (n. 2 and 3) in order to obtain a preliminary solution. This was then iteratively improved by the successive inclusion of the other pointings obtained at increasingly longer time intervals (in the following order: 4, 5, 6, 1). The phase-connected ephemeris of the six observations gave a period $P_{2011} = 13.18424736(16)$ s, which is within the errors of the much less accurate value measured in May 2008 ($P_{2008} = 13.18425(4)$ s, Mereghetti et al. 2011). A linear fit to these two values plus all the other period measurements (2002 May and September with *XMM-Newton* and November 1992 with *ROSAT*) gives the following limits on the period derivative: $-2.9 \times 10^{-13} < \dot{P} < 3.6 \times 10^{-13}$ s s $^{-1}$ (90% c.l.). We obtained a tighter constraint on \dot{P} by extending the phase-connected timing analysis to the 2008 data and fitting the pulse phases with a quadratic function: the results are $P = 13.1842474(2)$ s and $|\dot{P}| < 6 \times 10^{-15}$ s s $^{-1}$. The 2011 light curves folded at the spin period are shown in Fig. 4 for the soft and hard energy ranges. As in the previous observations, the light curve at low energy shows a strong nearly sinusoidal modulation (pulsed fraction $\sim 55\%$), while two peaks are visible above 0.5 keV.

Table 2. EPIC spectral results for the eclipse emission.

Parameter	Value
N_{H} (10^{20} cm $^{-2}$)	<2.9
Photon index	$1.87^{+0.22}_{-0.15}$
F_{PL}^a (10^{-14} erg cm $^{-2}$ s $^{-1}$)	7.3 ± 0.7
E_1 (keV)	0.43 (fixed)
I_1 (10^{-5} ph cm $^{-2}$ s $^{-1}$)	$1.1^{+0.7}_{-0.4}$
E_2 (keV)	0.5 (fixed)
I_2 (10^{-5} ph cm $^{-2}$ s $^{-1}$)	$0.68^{+0.29}_{-0.25}$
d.o.f.	35
χ^2_{ν}	1.16

^a Flux of the power-law component in the 0.2–10 keV range.

Table 3. EPIC spectral results for the uneclipsed emission.

	BB+PL	BB+Brem
N_{H} (10^{20} cm $^{-2}$)	1.6 ± 0.7	0.5 ± 0.5
kT_{BB} (eV)	30.6 ± 1.5	33.5 ± 1.3
R_{BB}^a (km)	66^{+67}_{-46}	35^{+30}_{-22}
Photon index	$1.96^{+0.11}_{-0.10}$	–
F_{PL}^b (10^{-13} erg cm $^{-2}$ s $^{-1}$)	$1.01^{+0.05}_{-0.03}$	–
kT_{Br} (keV)	–	$3.7^{+0.9}_{-0.7}$
F_{Br}^b (10^{-13} erg cm $^{-2}$ s $^{-1}$)	–	$0.78^{+0.06}_{-0.05}$
d.o.f.	262	262
χ^2_{ν}	1.27	1.42

^a Blackbody emission radius for $d = 650$ pc.

^b Flux in the range 0.2–10 keV.

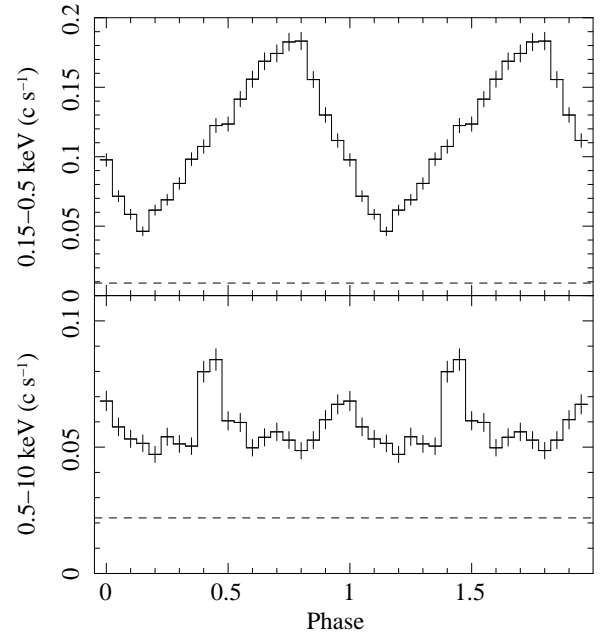


Fig. 4. EPIC pn light curve of RX J0648.0–4418 folded at the spin period in the soft (0.15–0.5 keV, top panel) and hard (0.5–10 keV, bottom panel) energy ranges. The dashed lines indicate the background level.

4. Discussion and conclusions

The presence of X-ray emission also during the eclipse, already noticed in May 2008, is confirmed by the new observations of HD 49798/RX J0648.0–4418, which show a spectrum characterized by strong N emission lines. A possible explanation is that these X-rays originate in HD 49798 itself, i.e. they are unrelated to the presence of a compact object in this system. This is particularly interesting since no O-type subdwarf has been detected in X-rays up to now⁵.

Our current understanding of the X-ray emission from early type stars is based on OB main sequence, giant and supergiant stars, which, compared to HD 49798, have very different luminosity, mass and composition. The X-ray emission of these stars originates in their strong, radiation-driven winds, where plasma is heated by shocks and instabilities (Pallavicini 1989). High resolution spectra of bright O type stars are characterized by

⁵ with the exception of BD +37° 442 (La Palombara et al. 2012). However, the possible presence of pulsations at 19 s suggests that also BD +37° 442 has a compact companion.

the presence of numerous emission lines (see, e.g. Kahn et al. 2001), but data with lower resolution and/or statistical quality are usually well fit by a combination of plasma emission models with different temperatures. The temperatures we derived are fully consistent with those found in a large sample of O stars studied with *XMM-Newton* (Nazé 2009). The luminosity of $\sim 3 \times 10^{30}$ erg s⁻¹ that we measured during the eclipse corresponds to an X-ray-to-bolometric flux ratio of $\sim 10^{-7}$, as typical O-type stars (Pallavicini 1989). Thus we conclude that the X-ray luminosity and spectrum observed during the eclipse are consistent with those of early type stars and support the interpretation of HD 49798 as the first hot subdwarf detected at X-ray energies.

In this respect it is interesting to note that HD 49798 is one of the few sdO stars for which evidence of wind mass loss has been reported (Hamann et al. 1981). This suggests that the processes responsible for X-ray emission in the stellar winds of massive O stars are also at work in the much weaker winds of hot subdwarfs and makes HD 49798 a particularly interesting target to explore the properties of radiatively driven winds through X-ray observations over a wide range of stellar parameters.

Thanks to the better coverage of the eclipse orbital phases, the new observations allowed us to study the eclipse shape. We derived a duration of 4311 ± 52 s for the total eclipse, consistent with the rough value of 4300 s that was estimated from the 2008 observation and used to constrain the system inclination in Mereghetti et al. (2009). We could also establish that the eclipse ingress and egress occur gradually. This can be explained if part of the X-ray emission originates in an extended region surrounding the compact object. It is easy to show with a simple geometrical model, based on the known orbital parameters and radius of HD 49798 ($1.45 R_{\odot}$, Kudritzki & Simon 1978), that the observed duration of ~ 500 s of the eclipse ingress and egress implies dimensions of the order of a few 10^4 km, much larger than the radius of a massive white dwarf (~ 3000 km). The presence of strong pulsations, which must necessarily originate close to the compact object, sets a limit on the flux coming from the extended region. Considering that $\sim 55\%$ of the counts below 0.5 keV are pulsed, this limit is of about 2×10^{-13} erg cm⁻² s⁻¹ (0.2–0.5 keV). A plausible scenario is that part of the high-energy radiation emitted by the compact object is scattered in the wind of HD 49798, as observed in more luminous X-ray binaries powered by wind accretion, such as, e.g., Vela X-1 or Cen X-3 (Sako et al. 1999; Ebisawa et al. 1996). This interesting possibility deserves to be explored with more sensitive X-ray observations with good spectral resolution (Sartore et al. in preparation).

The new observations confirm the stability in the long term properties of the X-ray emission from this binary system: the luminosity and pulse profile do not show significant variations compared to previous observations, but thanks to a better modeling of the eclipse spectrum we could obtain more accurate values for the spectral parameters of the uneclipsed emission. The lower temperature of the blackbody-like component, which dominates the low-energy pulsed emission, implies an emitting area difficult to reconcile with origin on the surface of a neutron star.

Thanks to a properly planned spacing of the observations, we could obtain for the first time a phase-connected timing solution for this system. This provides stronger constraints on the secular evolution of the 13 s spin period: the new limit on the period derivative, $|\dot{P}| < 6 \times 10^{-15}$ s s⁻¹ (90% c.l.), is more than two orders of magnitude smaller than the previous value (-5×10^{-13} s s⁻¹ $< \dot{P} < 9 \times 10^{-13}$ s s⁻¹, Mereghetti et al. (2011)). Considering the small torque expected for the low ac-

cretion rate onto this pulsar, this limit is still insufficient to definitely rule out a neutron star, a possibility not dismissed yet, although we believe that the observed X-ray luminosity and spectrum are best explained by a white dwarf companion. In this respect it is essential to extend the phase-connected solution over a longer time span by means of new X-ray measurements of the spin period.

Acknowledgements. This work is based on observations obtained with *XMM-Newton*, an ESA science mission with instruments and contributions directly funded by ESA Member States and NASA. We acknowledge financial contributions by the Italian Space Agency through ASI/INAF agreements I/009/10/0 and I/032/10/0 and by INAF through PRIN INAF 2010.

References

- den Herder, J. W., Brinkman, A. C., Kahn, S. M., et al. 2001, *A&A*, 365, L7
 Ebisawa, K., Day, C. S. R., Kallman, T. R., et al. 1996, *PASJ*, 48, 425
 Hamann, W. 2010, *Ap&SS*, 119
 Hamann, W., Gruschinske, J., Kudritzki, R. P., & Simon, K. P. 1981, *A&A*, 104, 249
 Israel, G. L., Stella, L., Angelini, L., et al. 1997, *ApJ*, 474, L53
 Kahn, S. M., Leutenegger, M. A., Cottam, J., et al. 2001, *A&A*, 365, L312
 Kudritzki, R. P. & Simon, K. P. 1978, *A&A*, 70, 653
 La Palombara, N., Mereghetti, S., Tiengo, A., & Esposito, P. 2012, *ApJ*, 750, L34
 Mereghetti, S., La Palombara, N., Tiengo, A., et al. 2011, *ApJ*, 737, 51
 Mereghetti, S., Tiengo, A., Esposito, P., et al. 2009, *Science*, 325, 1222
 Nazé, Y. 2009, *A&A*, 506, 1055
 Pallavicini, R. 1989, *A&A Rev.*, 1, 177
 Perryman, M. A. C. & ESA, eds. 1997, *ESA Special Publication*, Vol. 1200, The HIPPARCOS and TYCHO catalogues. Astrometric and photometric star catalogues derived from the ESA HIPPARCOS Space Astrometry Mission
 Sako, M., Liedahl, D. A., Kahn, S. M., & Paerels, F. 1999, *ApJ*, 525, 921
 Strüder, L., Briel, U., & Dennerl, K. e. 2001, *A&A*, 365, L18
 Thackeray, A. D. 1970, *MNRAS*, 150, 215
 Turner, M. J. L., Abbey, A., Arnaud, & et al. 2001, *A&A*, 365, L27
 Wang, B. & Han, Z. 2010, *Research in Astronomy and Astrophysics*, 10, 681